Journal of Applied Electrochemistry (2006) 36:603–608
DOI 10.1007/s10800-005-9113-8

Dissolution kinetics of WO_3 in acidic solutions

MUSTAFA ANIK[1,2,*] and TUBA CANSIZOGLU[1]
[1]*Metallurgy Institute, Osmangazi University, 26480, Eskisehir, Turkey*
[2]*Department of Metallurgical and Materials Engineering, Eskisehir Osmangazi University, 26480, Eskisehir, Turkey*
*(*author for correspondence, e-mail: manik@ogu.edu.tr)*

Received 11 February 2005; accepted in revised form 20 December 2005

Key words: CMP, dissolution kinetics, rate constant, tungsten, tungsten oxide

Abstract

Potentiostatic polarization and rotating disk electrode techniques were used to obtain the rate constant for the dissolution of electrochemically-formed (at 1 V) WO_3 on tungsten (W) in acidic solutions. The corresponding rate constant for the chemical dissolution of WO_3(s) powder was found by measuring the dissolved tungsten concentration as a function of time and pH. The chemical dissolution experiments supported the view that the rate-determining step in the anodic reaction of W in acidic solution is the chemical dissolution of WO_3(s) formed on the metal surface. Zeta potential measurements gave the isoelectric point (iep) of the WO_3(s) powder as pH 1.5, a value that was somewhat smaller than the point of zero charge (pzc) of WO_3(s) formed on W metal (pH 2.5). This difference was attributed to the highly hydrated nature of the oxide film formed on W metal in aqueous systems.

1. Introduction

Chemical–mechanical polishing (CMP) is now firmly established as a key planarization technique in semiconductor process technology [1]. Among the most widespread applications of CMP is the planarization of tungsten (W) and interlayer dielectric (IDL). In the case of W, it has been proposed that the CMP process proceeds via successive steps of surface oxide (passivating layer) formation and oxide removal [2], although the detailed mechanisms remain unresolved [2–9]. As device features continue to shrink, the need to control the metal removal process at the nanometer scale becomes critical. This new process control challenge requires that the anodic behavior of tungsten be better understood so that appropriate molecular-level rate laws can be developed.

The rate-determining step for tungsten (W) reaction in acidic solution is believed to involve the chemical dissolution of WO_3(s) formed on the metal surface [10–17]. However, this conclusion has not yet had the benefit of supporting experimental data from the direct chemical dissolution of tungstic oxide. Heumann and Stolica [11], and Armstrong et al. [12] provided some reports on this issue to support their electrochemical dissolution results in alkaline solutions. Nevertheless, their investigations were not systematic (no precise powder surface area measurement, no analysis of the solution for the dissolved metal concentration). In the hydrometallurgical extraction literature there are some reports on the chemical dissolution behavior of WO_3(s) in alkaline solution [18, 19]. In contrast, no comparable information is available for acidic solution, although the stability of this oxide in low pH environments is important for CMP as well as other technologically important processes [1–9, 20].

In this study, potentiostatic polarization experiments with a rotating disk electrode are performed in 0.1 M H_3PO_4 buffered solutions in order to obtain the dissolution rate constant of the electrochemically formed WO_3 (on the metallic W) in acidic solution. Chemical dissolution experiments of WO_3(s) powder are also conducted in the same acidic solution and the dissolution rate data for WO_3(s) powder are compared with results of electrochemical experiments with metallic W.

2. Background: anodic behavior of tungsten in acidic solution

In our previous work [20, 21] the effect of pH on the anodic behavior of tungsten was investigated over a wide pH range (pH 0.5–13):

Total anodic oxidation reaction of W in acidic and weakly-alkaline solutions can be expressed as:

$$W + 3H_2O = WO_3(s) + 6H^+ + 6e^- \quad (1)$$

This oxidation reaction is followed by slow dissolution of the oxide phase. Below pH 1 dissolution is assisted by H^+ ions:

$$WO_3(s) + H^+ \rightarrow WO_2OH^+(aq) \quad (2)$$

In the vicinity of pH 2.5, which is identified as the point of zero charge (pzc) of the surface W oxide, dissolution is H_2O-assisted as:

$$WO_3(s) + H_2O \rightarrow WO_3.H_2O(s) = H_2WO_4(aq) \quad (3)$$

Above the pzc, OH^--assisted dissolution is the main dissolution pathway (Equation 4) in acidic solutions:

$$WO_3(s) + OH^- \rightarrow WO_4^{2-}(aq) + H^+ \quad (4)$$

The dissolution rates (R) for the reactions in Equations 2, 3 and 4 can be expressed as:

$$R_H = k_H C_H \quad (5)$$

$$R_W = k_W \quad (6)$$

$$R_{OH} = k_{OH} C_{OH} \quad (7)$$

where k_H, k_W and k_{OH} are rate constants for H^+-assisted, H_2O-assisted and OH^--assisted dissolutions, respectively, C_H and C_{OH} are bulk H^+ and OH^- concentrations, respectively. Above the anodic potentials at which WO_3 coats W surface completely ([20]; above 300 mV; pseudo-plateau region), the anodic reaction rate of W is controlled by the chemical reactions in Equations 2, 3 and 4 ([20]; the rate determining steps). Therefore, at these potentials the steady-state W anodic current, which reflects the total rate, can be expressed in acidic solutions as:

$$\frac{i}{nF} = k_H C_H + k_W + k_{OH} C_{OH} \quad (8)$$

where i is the steady-state anodic current density, n is the total number of electrons involved in the anodic reaction of W (Equation 1), F is Faraday constant. Equation 8 is also called rate law for the dissolution of electrochemically-formed WO_3 on the W surface in acidic solutions.

3. Materials and methods

A tungsten (W) rod 0.4 cm in diameter (99.99% purity) and WO_3(s) powder (99.99% purity) were obtained from Aldrich. The average size of the WO_3(s) particles was 20 μm (supplier information). The surface area of the powders was measured by B.E.T. as 1.1 $m^2\ g^{-1}$. Reagent grade H_3PO_4, H_2SO_4, KOH and K_2SO_4 were purchased from Aldrich. All the aqueous solutions were prepared from doubly distilled water.

For the electrochemical experiments the water was deoxygenated by bubbling argon and purging was continued throughout the experiments. The test solutions were buffered using 0.1 M H_3PO_4, and pH was adjusted with H_2SO_4 or KOH. Ionic strength was fixed by adding required amount of K_2SO_4.

The W electrode used in the electrochemical experiments was embedded in a cylindrical piece of Teflon. To block the crevice between the Teflon holder and the electrode, epoxy was applied and subsequently allowed to harden in vacuum. The exposed electrode surface (0.126 cm^2) was ground with 1200 grit grinding paper and polished with 1 μm diamond paste just prior to each experiment.

A standard three-electrode system consisting of a working electrode (tungsten), a counter electrode (carbon rod), and a reference electrode (saturated calomel electrode) was used. A Gamry model PC4/300 mA potentiostat/galvanostat controlled by a computer with a model DC105 DC Corrosion Analysis software was used in the electrochemical measurements. Rotating disc electrode (RDE) experiments were carried out using an EG&G model 616 rotating assembly. The electrical connection was provided from the back of the electrode by attaching it to the RDE assembly. All experiments were performed in 800 ml glass cell.

Potentiostatic polarization was generated at 1 V (SCE) under rotation which was varied between 0 and 2500 rpm (0, 300, 500, 1000, 1500, 2000 and 2500 rpm). After each rpm increment, electrode was held at the working electrode long-enough to obtain steady anodic current. Unless indicated otherwise all potentials are referred to the saturated calomel reference electrode, SCE (SCE, +0.241 V vs. SHE).

The chemical dissolution experiments were carried out in a 1 l plastic vessel filled with 500 ml of 0.1 M H_3PO_4 aqueous solution. The initial amount of WO_3(s) powder was 10 g in each test solution (20 g WO_3(s) powder per liter). A two-bladed agitator was used to mix the solution; the agitation rate was 400 rpm. Approximately 10 ml of solution samples were drawn from the reactor at desired time intervals. Each sample was immediately filtered (to prevent continued reaction), placed in an air-tight sample bottle and later analyzed for its metal content using a Optima 2100 DV inductively coupled plasma (ICP) optic emission spectrophotometer. This device had the ability to measure the amount of W in solution down to 0.1 ppm.

The zeta potentials of WO_3(s) particles were measured as a function of pH at room temperature (25 °C) by using a Coulter Delsa 440SX electrophoretic light scattering analyzer. The pH of the solution was adjusted with HNO_3 and the pH measurements were carried out by Thermo Orion Model 525A Meter (pH range: −2.0 to 19.9 and pH resolution: 0.001) with non – glass electrode. The powders were kept in 10^{-3} M KNO_3 solutions (at pHs 1 to 3.5) for 12 h before the measurements.

All experiments were conducted at laboratory temperature (25 ± 1 °C).

4. Results and discussion

4.1. *Potentiostatic polarization experiments with rotating disk electrode*

The steady-state anodic currents obtained at 1 V for specimen rotations 0, 300, 500, 1000, 1500, 2000 and 2500 rpm are shown in Figure 1(a–c) for various pH values. As the pH increases (up to pH 1.5), the steady-

state current decreases in Figure 1(a). The steady-state current reaches its lowest value at around pH 2.1 in Figure 1(b) and as the pH increases (above pH 2.1) the steady-state current also increases in Figure 1(b, c).

The rotation dependence of the steady-state current at each pH can be shown better in the form of Koutecky–Levich (i^{-1} vs. $w^{-1/2}$; w is an angular velocity [22, 23]) plots as given in Figure 2(a–c). These plots are defined by Equation 9 for a first order reaction [22, 23]:

$$\frac{1}{i} = \frac{1}{i_K} + \frac{1}{i_D} \tag{9}$$

where i_K and i_D represent the kinetic- and diffusion-limited parts of the anodic current, respectively. Extrapolation of the steady-state currents to infinite rotation speed ($w \to \infty$) provides kinetic currents for each pH value in Figure 2(a–c) (The inverse value of the kinetic current for each pH value can be red on these figures). By the use of data in Figure 2(a–c), the pH dependence of the kinetic current can be illustrated as in Figure 3. The shape of steady-state kinetic current in Figure 3 results from the competition in between reactions in Equations 2, 3 and 4 depend on the solution pH [20, 21].

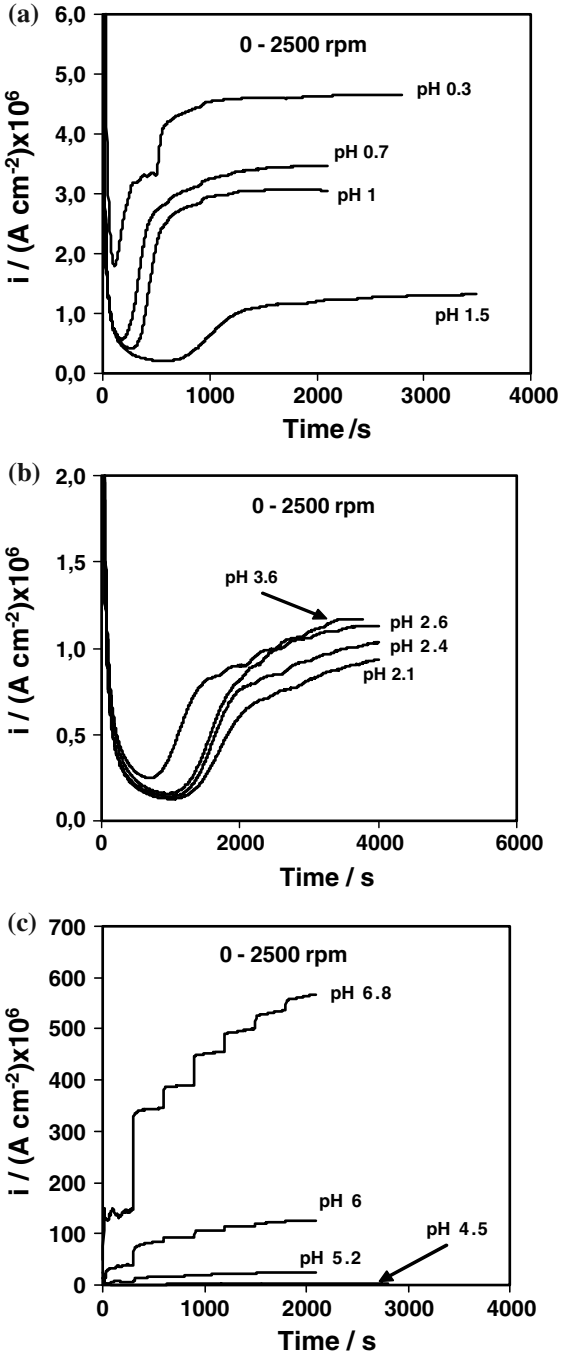

Fig. 1. Steady-state currents for W obtained at pH (a) 0.3, 0.7, 1, 1.5; (b) 2.1, 2.4, 2.6, 3.6; (c) 4.5, 5.2, 6, 6.8.

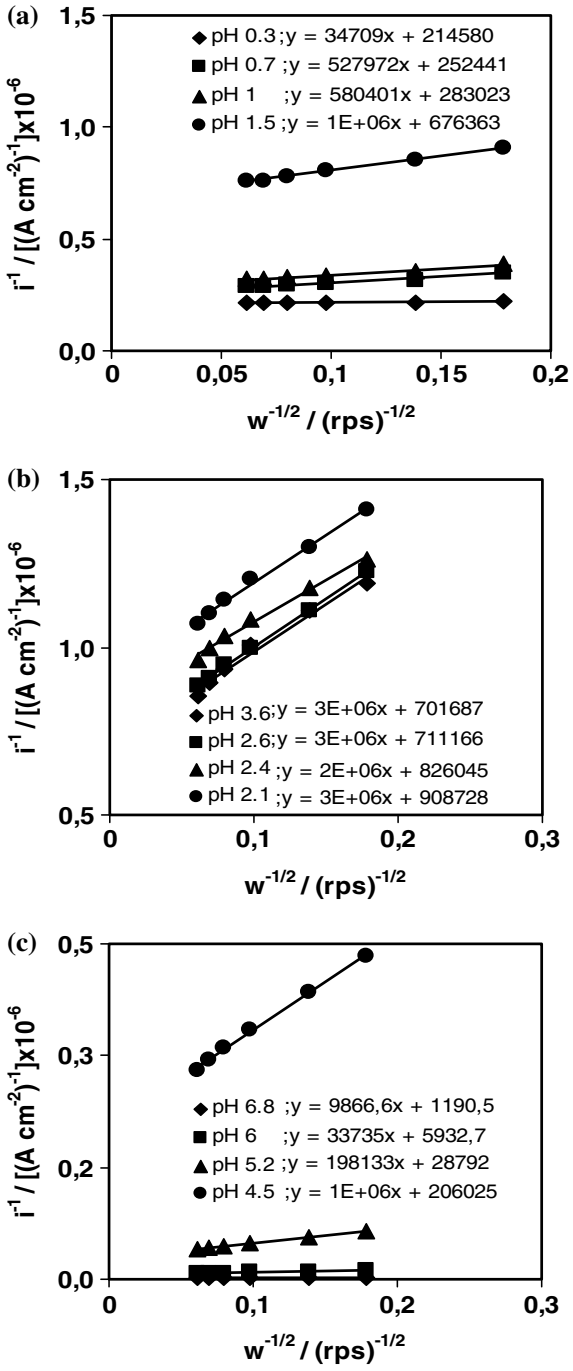

Fig. 2. Rotation dependence of the steady-state anodic current in the form of Koutecky Levich plots for pH (a) 0.3, 0.7, 1, 1.5; (b) 2.1, 2.4, 2.6, 3.6; (c) 4.5, 5.2, 6, 6.8.

The data (big circles) in Figure 3 can be fitted by Equation 8 as shown by the solid line on figure. The data fit provides the following rate constants:

$$\frac{k_H}{\gamma_H} = 2.5 \times 10^{-11}\,\mathrm{cm\,s^{-1}} \tag{10}$$

$$k_W = 1.8 \times 10^{-12}\,\mathrm{mol\,cm^{-2}\,s^{-1}} \tag{11}$$

$$\frac{k_{OH}}{\gamma_{OH}} = 2.2 \times 10^{-2}\,\mathrm{cm\,s^{-1}} \tag{12}$$

where γ_H and γ_{OH} are activity coefficients for H^+ and OH^-, respectively. The values of activity coefficients are depend on the ionic strength of solution.

The dashed (–) line on Figure 3 (with the nearby equation) shows the fit of data according to Equation 8 if only the OH^- - assisted dissolution (with $k_{OH} = 0.022$ cm s^{-1}) is considered (k_H and k_W are substituted by zero in Equation 8). The slope of this dashed line shows that the dissolution reaction order of W with respect to OH^- ion is 1 [20]. Since the W CMP is carried out at pH 4 (1–9), OH^- - assisted dissolution is the main concern in this investigation. Therefore, the chemical dissolution experiments are performed in the pH range corresponding to the OH^--assisted dissolution range of the W.

4.2. *Chemical dissolution of WO_3(s) powder*

The experimental data obtained for WO_3 dissolution for pH 4, 5 and 6 are provided in Figure 4. For each pH the W concentration in solution increases almost linearly with time up to 8 h. Upon each unit increment of pH (from pH 4 to 6), the concentration of W increases by almost one decade. The chemical dissolution rate of WO_3(s) can be expressed as:

$$\frac{dC_W}{dt}\frac{1}{A} = k_{OH} C_{OH}^{m} \tag{13}$$

where C_W is the concentration of dissolved W (mol cm^{-3}), t is the time (second), A is the surface area of WO_3(s) powder (cm^2 g^{-1}), k_{OH} is the apparent rate constant for Reaction 4 (cm s^{-1}; the left hand side of the equation is multiplied by 50 cm^3 g^{-1} since 10 g powder is used in 500 cm^3 test solution), C_{OH} is the bulk concentration of OH^- ions (mol cm^{-3}) and m is the reaction order for OH^-.

Since in these experiments the dissolved amount of W is very low, as compared to the initial amount of W (as WO_3(s) powder), the change in the surface area (A) of the powder during dissolution is negligible. For example, the maximum amount of dissolved W was 169 ppm (0.92 mM) at pH 6 after 8 h. If the initial WO_3(s) powder (10 g) dissolved completely, the amount of W (7.93 g) in solution would be 7930 ppm (43.1 mM). Thus, the amount of dissolved W was only about 2%. Therefore, Equation 13 can be used in the calculation of the various kinetic parameters by keeping the A value constant (initial A is 1.1 m^2 g^{-1}).

The rate constant k_{OH} and the reaction order, m, are determined by rewriting Equation 13 as:

$$\log\left(\frac{dC_W}{dt}\frac{1}{A}\right) = \log k_{OH} + m \log C_{OH} \tag{14}$$

Figure 5 presents a plot of log ($dC_W/dt \cdot 1/A$) vs. log C_{OH}; the dC_W/dt values are taken from the slopes in Figure 4 for each pH value. The reaction order for OH^-

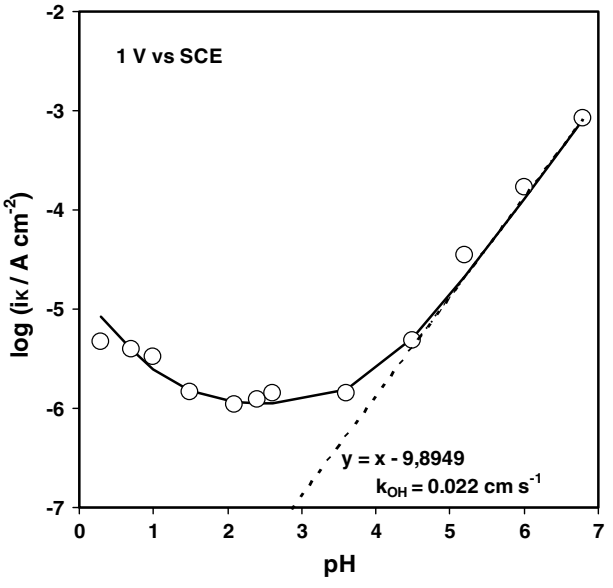

Fig. 3. The pH dependence of the steady-state kinetic currents (obtained at 1 V vs. SCE) of W in acidic solution. The experimental data points (big circles) are fitted according to Equation 8 (solid – line) and the corresponding rate constants are collected as in Equations 10, 11 and 12. Dashed (–) line (with the nearby equation) shows the fit of data according to Equation 8 if only the OH^--assisted dissolution (with $k_{OH} = 0.022$ cm s^{-1}) is considered.

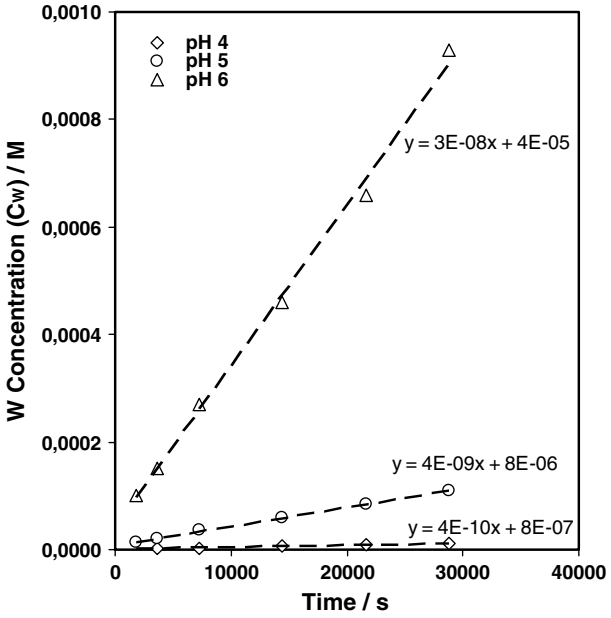

Fig. 4. The effect of pH on the dissolution rate of WO_3 particles at 25 °C with 400 rpm solution stirring.

in Figure 5 ($m = 0.937$) is very close to 1 as in the case in Figure 3 (slope of dashed (–) line). The apparent rate constant (k_{OH}) obtained from Figure 5 is 3×10^{-3} cm s^{-1}. This rate constant value is about 7.5 fold lower than that obtained by the electrochemical technique (Figure 3; 2.2×10^{-2} cm s^{-1}). This difference may partly be due to different experimental techniques. Another reason may be the difference in the characteristics of the powder WO_3(s) and the oxide film formed on the metallic W. Initially in the chemical dissolution experiments we observed that there was no effect of solution stirring rate on the powder dissolution rate. In other words, powder dissolution is totally kinetically controlled and there is no diffusion effect. This observation is also reported for WO_3(s) powder dissolution in alkaline solutions [19].

4.3. *Zeta potential of WO_3(s) powder*

The effect of pH on the zeta potential of the WO_3(s) powder used in the dissolution experiments is shown in Figure 6. The isoelectric point (iep; the pH at which zeta potential is zero) of WO_3(s) occurs around pH 1.5. This iep value is comparable with literature values; the iep for WO_3(s) is reported by Parks [24] to be in the range of pH 0.4–1. (Specific adsorptions in different salts and the addition of a large amount of an acid to the solutions that causes uncontrolled changes in the ionic strengths may result in variations in the measured iep values of WO_3(s) powder). It appears, however, that the iep of WO_3(s) powder is somewhat less than the pzc (the pH at which surface potential is zero) observed for the oxide film on W. As already noted above in connection with Figure 3, the pH associated with the current minimum (i.e., pH 2.5) can be taken to represent the pzc of the surface oxide formed on W (20). The same pzc value (pH = 2.6) was identified by Macdonald et al. [25] who determined steady-state currents on W at 10 V in H_3PO_4/NaOH buffer solutions. Also, Raghunath et al. [5] obtained an isoelectric point of pH 2.3 for W powder by the electrokinetic measurements in 10^{-3} M KNO_3 solution, suggesting that the powder had a surface coating of tungsten oxide.

The pzc of oxides depends on several physicochemical properties of the oxide phase [24, 26, 27]: (a) The stoichiometry of the oxide, (b) the crystal structure, (c) the degree of surface hydration, (d) the difference in the acidic and basic dissociation constants of the surface hydroxyl groups. Among these, the degree of surface hydration may explain why the iep observed for WO_3(s) powder (pH 1.5) is different from the pzc observed for the oxide formed on W metal in aqueous solution (pH 2.5). The oxide films formed on W in aqueous solution can be expected to be more hydrated with respect to WO_3(s) powders. In fact, it is reported (through in situ surface enhanced Raman spectroscopy characterization of the W surface in acidic solution) that the anodic oxide film is hydrated and the extent of hydration increases with anodic polarization [17]. Upon hydration H_2O molecules are substituted for O^{2-} or OH^- ions bound to the oxide surface, and the surface becomes more positive (less acidic; more protonated). Thus, the pzc shifts to higher pH values [25, 28, 29]. Probably due to this reason the pzc for WO_3(s) formed on W in electrochemical experiments shifts to pH 2.5. Also the conditions in the zeta potential measurements are not exactly the same with those in the dissolution experiments and there may be a difference in the intensity of the specific adsorptions on the oxide surface in both cases. Therefore, the difference in the intensity of the specific adsorption may contribute to the difference between the iep and pzc. It is also reported that [30] the phosphate ions, which are incorporated in the WO_3(s) film during the dissolution experiments but not during

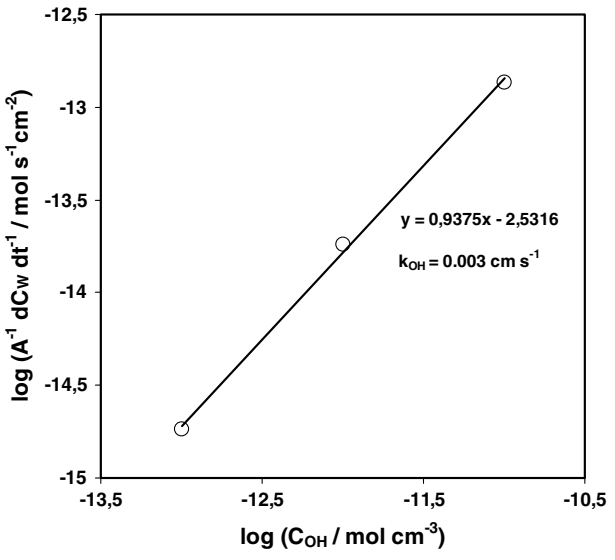

Fig. 5. Estimation of the reaction order for OH^-, and the apparent rate constant (k_{OH}) according to Equation 14.

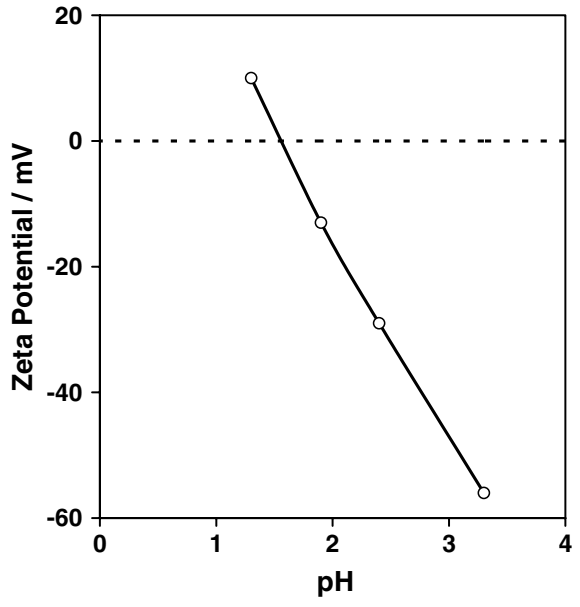

Fig. 6. The zeta potential of WO_3(s) powder as a function of pH.

the case zeta potential measurements, may change slightly the composition of the oxide film.

5. Summary and conclusions

In this investigation the chemical dissolution rate determining step in the total anodic reaction of W in acidic solutions was verified by comparing the dissolution rate constants obtained by electrochemical and chemical techniques. Conclusions arising from this work are summarized below:

- The OH^--assisted dissolution rate constant for metallic W was obtained as 2.2×10^{-2} cm s^{-1}. The corresponding rate constant for WO_3(s) powder dissolution was 3×10^{-3} cm s^{-1}. Both electrochemical and chemical techniques showed that the reaction order for OH^- ion was 1. These observations support the view that the rate-determining step in the reaction of W in acidic environment is the chemical dissolution of WO_3(s) formed on the metal surface.
- The iep of WO_3(s) powder ($\sim$pH 1.5) was found to differ somewhat from the pzc of WO_3(s) formed on W metal ($\sim$pH 2.5). This difference is attributable to the highly hydrated nature of the oxide film formed on W in aqueous systems. This difference was also assumed as the main reason for the higher dissolution rate constant of the electrochemically formed WO_3(s).

References

1. J.M. Steigerwald, S.P. Murarka and R.J. Gutmann, *Chemical Mechanical Planarization of Microelectronic Materials* (Wiley, New York, 1997), p. 1.
2. F.B. Kaufman, D.B. Thompson, R.E. Broadie, M.A. Jaso, W.L. Guthrie, D.J. Pearson and M.B. Small, *J. Electrochem. Soc.* **138** (1991) 3460.
3. E.A. Kneer, C. Raghunath, S. Raghavan and J.S. Jeon, *J. Electrochem. Soc.* **143** (1996) 4095.
4. S. Basak, K. Mishra, B. Withers and K. Rajeshwar, *in* S. Raghavan and I. Ali (Eds), *First Int. Symp. Chemical Mechanical Planarization,* Vol. 96-22 (Electrochem. Soc. Proc., Pennington, NJ, 1997) p. 137.
5. C. Raghunath, K.T. Lee, E.A. Kneer, V. Mathew and S. Raghavan, *in* S. Raghavan and I. Ali (Eds), *First Int. Symp. Chemical Mechanical Planarization,* Vol. 96-22 (Electrochem. Soc. Proc., Pennington, NJ, 1997) p. 1.
6. E.A. Kneer, C. Raghunath, V. Mathew, S. Raghavan and J.S. Jeon, *J. Electrochem. Soc.* **144** (1997) 3041.
7. D.J. Stein, D. Hetherington, T. Guilinger and J.L. Cecchi, *J. Electrochem. Soc.* **145** (1998) 3190.
8. D.J. Stein, D. Hetherington and J.L. Cecchi, *J. Electrochem. Soc.* **146** (1999) 376.
9. D. Tamboli, S. Seal and V. Desai, *J. Vac. Sci. Technol.* **A17** (1999) 1168.
10. J.W. Johnson and C.L. Wu, *J. Electrochem. Soc.* **118** (1971) 1909.
11. T. Heumann and N. Stolica, *Electrochim. Acta* **16** (1971) 1635.
12. R.D. Armstrong, K. Edmonson and R.E. Firman, *J. Electroanal. Chem.* **40** (1972) 19.
13. M.R. Arora and R. Kelly, *Electrochim. Acta* **19** (1974) 413.
14. M.R. Arora and R. Kelly, *J. Electrochem. Soc.* **124** (1977) 1493.
15. F. Di Quarto, A. Di Paola and C. Sunseri, *J. Electrochem. Soc.* **127** (1980) 1016.
16. F. Di Quarto, A. Di Paola and C. Sunseri, *Electrochim. Acta* **26** (1981) 1177.
17. R.S. Lillard, G.S. Kanner and D.P. Butt, *J. Electrochem. Soc.* **145** (1998) 2718.
18. J.W. Van Put, W.P.C. Duyvesteyn and F.G.J. Luger, *Hydrometallurgy* **26** (1991) 1.
19. J.W. Van Put and P.M. De Koning, *Hydrometallurgy* **28** (1992) 353.
20. M. Anik and K. Osseo-Asare, *J. Electrochem. Soc.* **149** (2002) B224.
21. M. Anik, T. Cansızoglu and S. Cevik, *Turk. J. Chem.* **28** (2004) 425.
22. Yu.V. Pleskov and V.Yu. Filinovskii, *The Rotating Disc Electrode* (Plenum, New York, 1976), p. 1.
23. A.J. Bard and L.R. Faulkner, *Electrochemical Methods Fundamentals and Applications*, 2nd edn., (John Wiley, New York, 2001), p. 331.
24. G.A. Parks, *Chem. Rev.* **65** (1965) 177.
25. D.D. Macdonald, E. Sikora and J. Sikora, *Electrochim. Acta* **43** (1998) 2851.
26. S.M. Ahmed, *in* J.W. Diggle (Ed), 'Oxides and Oxide Films', Vol. 1, (Marcel Dekker, New York, 1972) p. 319.
27. W. Stumm, *Chemistry of the Solid – Water Interface* (John Wiley, New York, 1992), p. 157.
28. D.J. O'Connor, P.G. Johansen and A.S. Buchanan, *Trans. Faraday Soc.* **52** (1956) 229.
29. M. Robinson, J.A. Pask and D.W. Fuerstenau, *J. Am. Ceram. Soc.* **47** (1964) 516.
30. M. Metikos-Hukovic and Z. Grubac, *J. Electroanal. Chem.* **556** (2003) 167.